iScience, Volume *23*

Supplemental Information

Antispasmodic Drug Drofenine as an Inhibitor of Kv2.1 Channel Ameliorates Peripheral Neuropathy in Diabetic Mice

Xiaoju Xu, Xu Xu, Yanping Hao, Xialin Zhu, Jian Lu, Xingnan Ouyang, Yin Lu, Xi Huang, Yang Li, Jiaying Wang, and Xu Shen

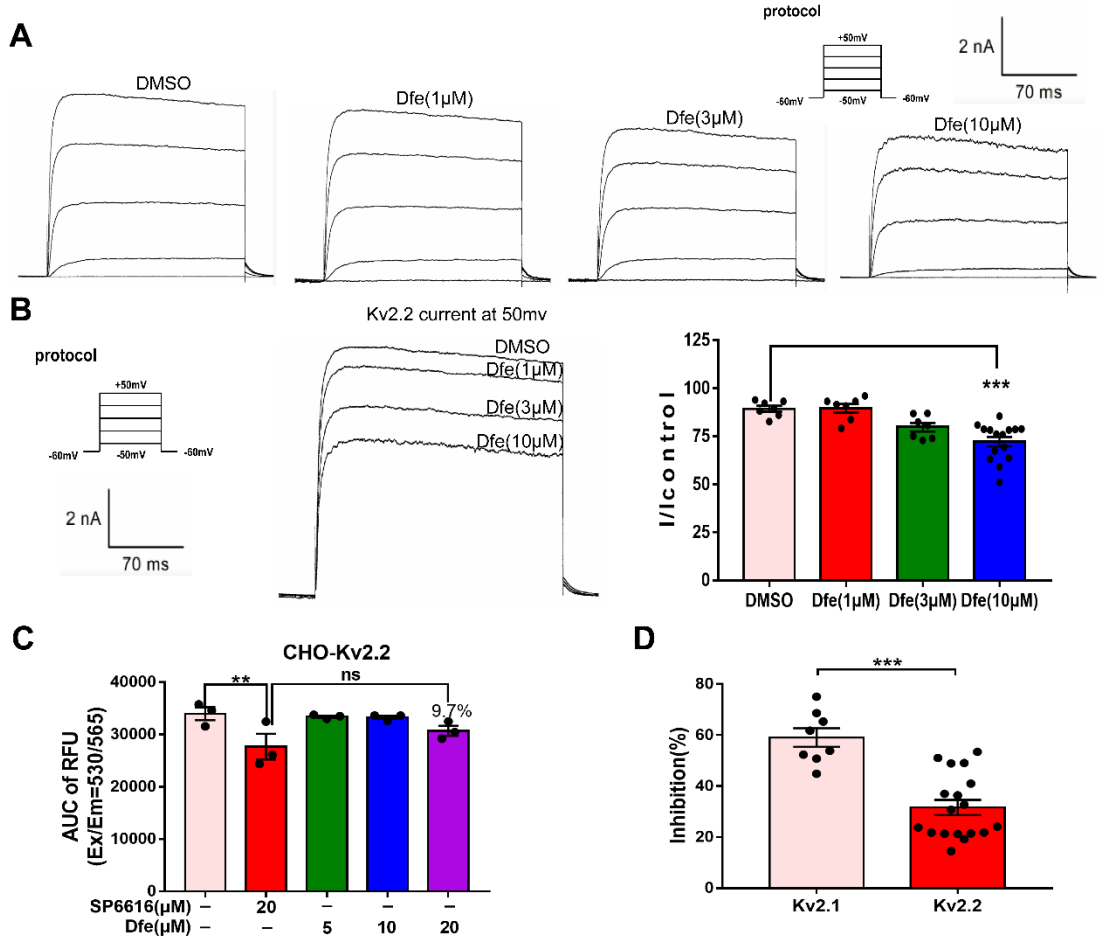

Supplemental Fig. S1. Dfe exhibits selectivity for Kv2.1 over Kv2.2, related to Figure 1.

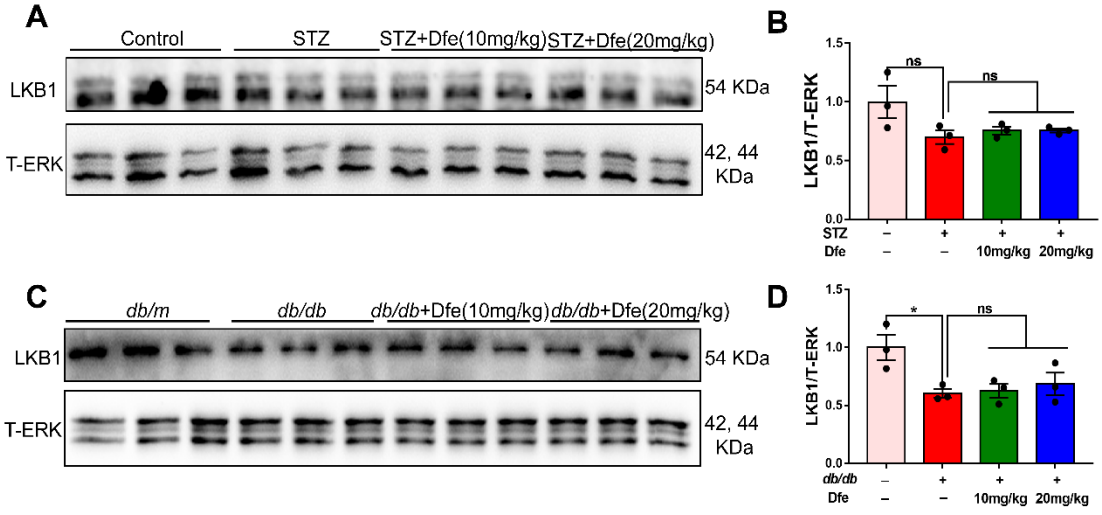

Supplemental Fig. S2. Western blot results of LKB1 protein expression in DPN

mice, related to Figure 5.

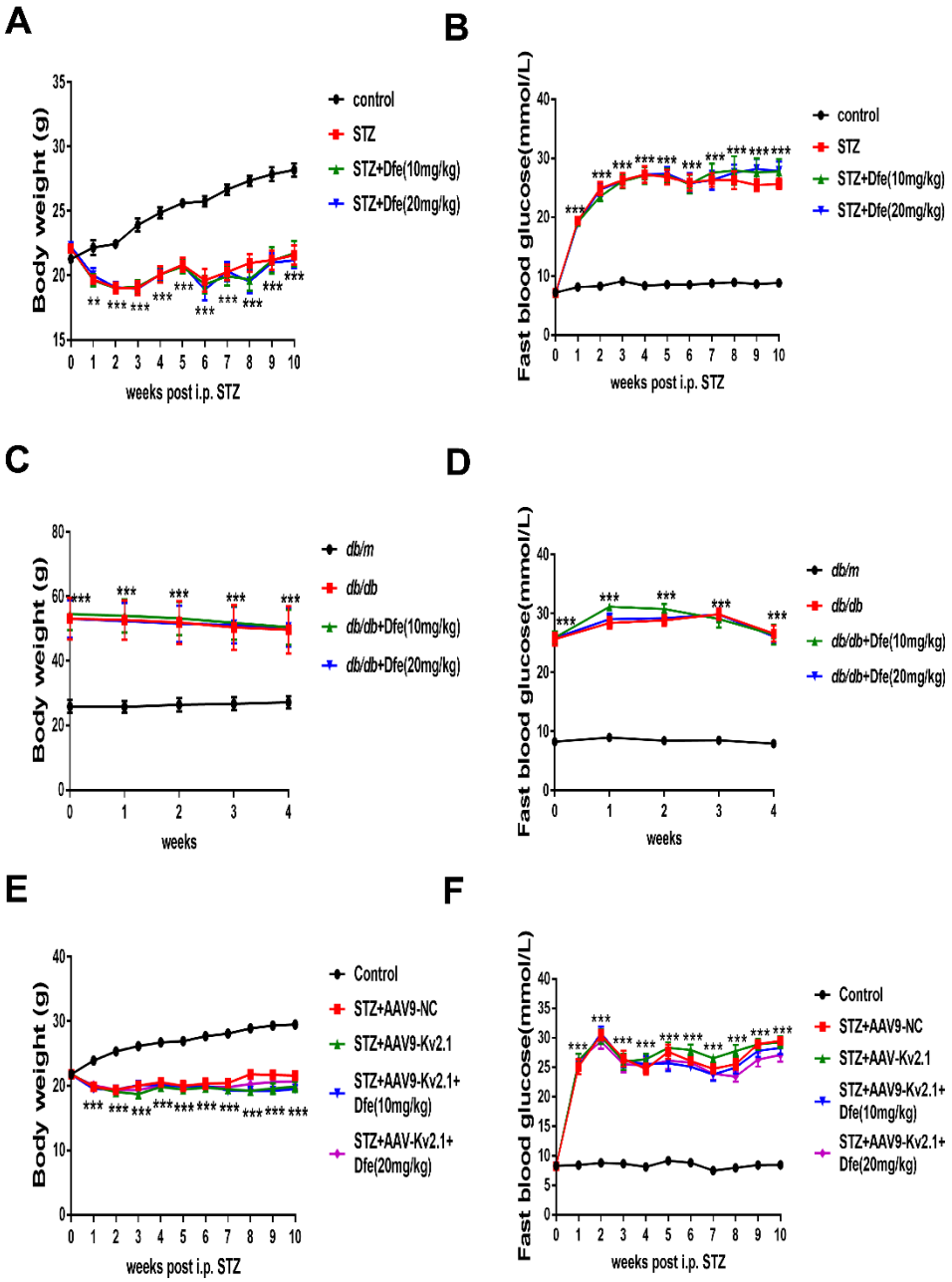

Supplemental Fig. S3. Time course of body weight and fast blood glucose in DPN mice, related to Figure 4.

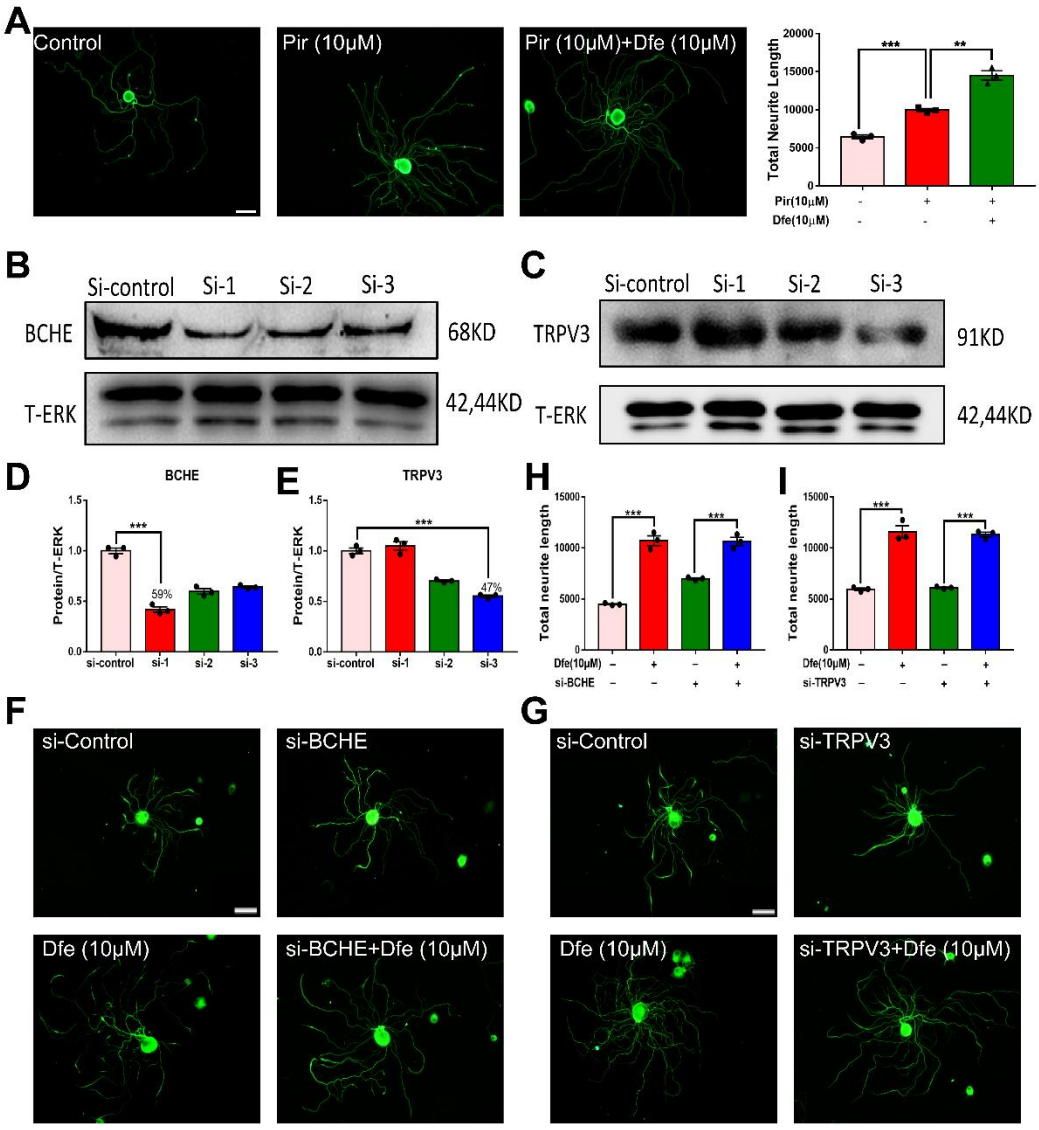

Supplemental Fig. S4. Dfe did not promoted neurite outgrowth of DRG neuron in DPN mice through BCHE and TRPV3, related to Figure 3.

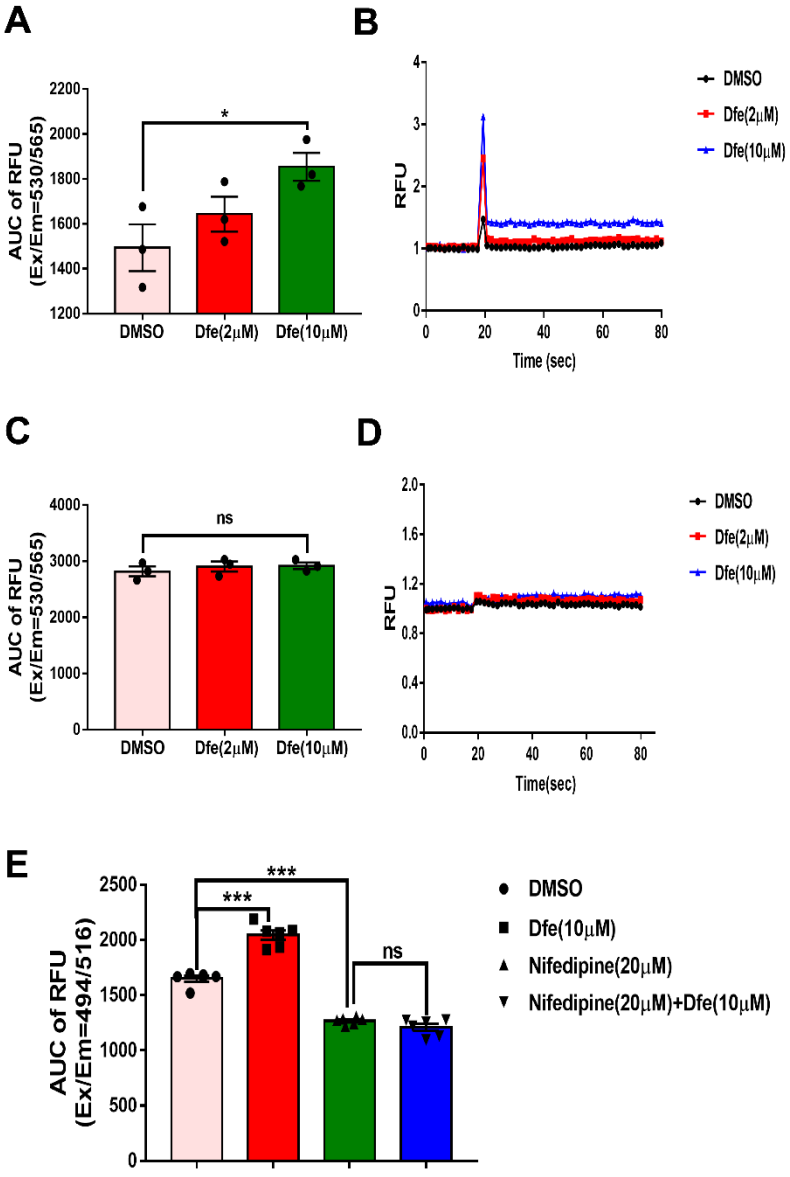

Supplemental Fig. S5. Dfe increased calcium influx in DRG neuron, related to Figure 5.

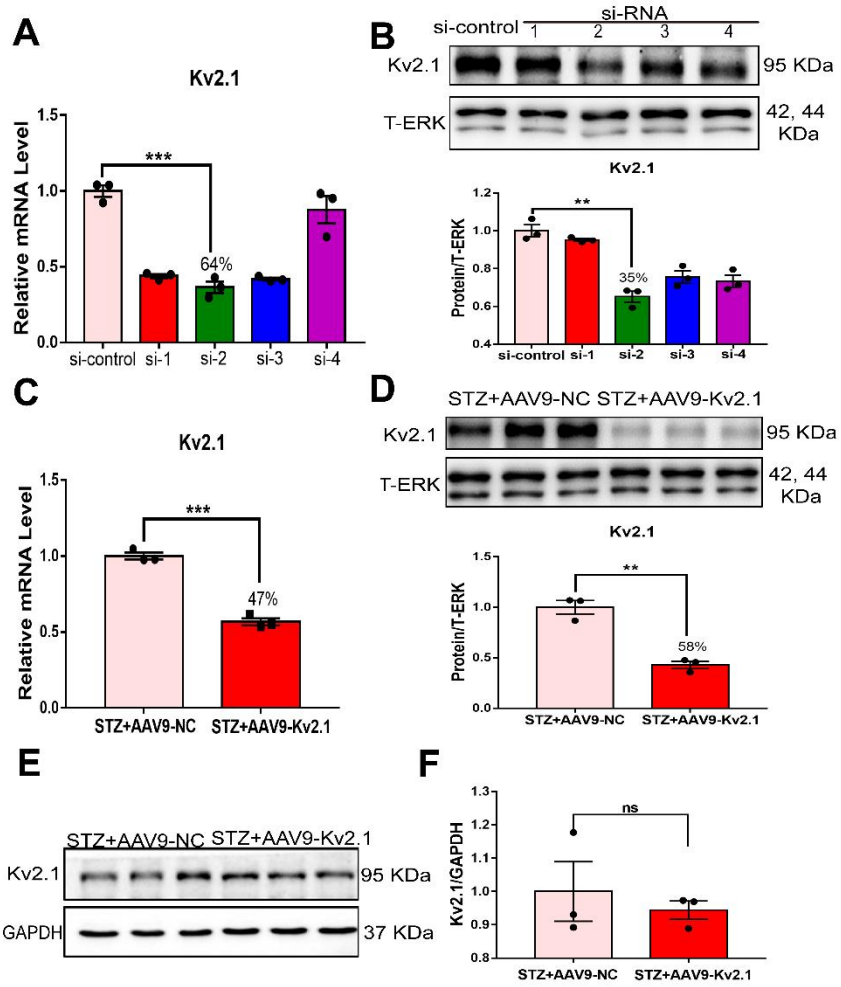

Supplemental Fig. S6. Screen of Kv2.1 interference sequence and identification of Kv2.1 protein expression, related to Figure 3-8.

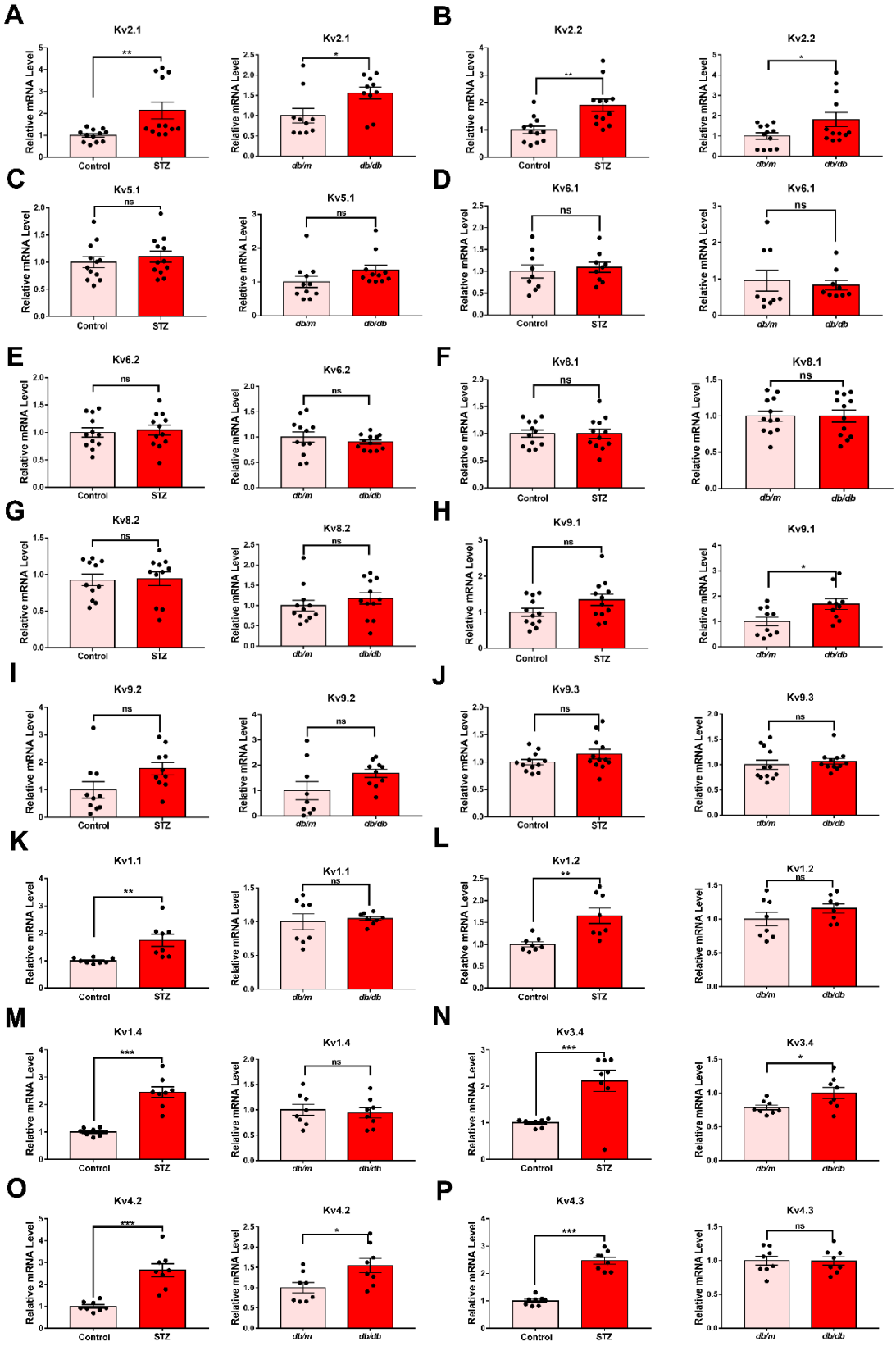

Supplemental Fig. S7. Transcription analyses of Kv channel in DRG tissue of DPN mice, related to Figure 2.

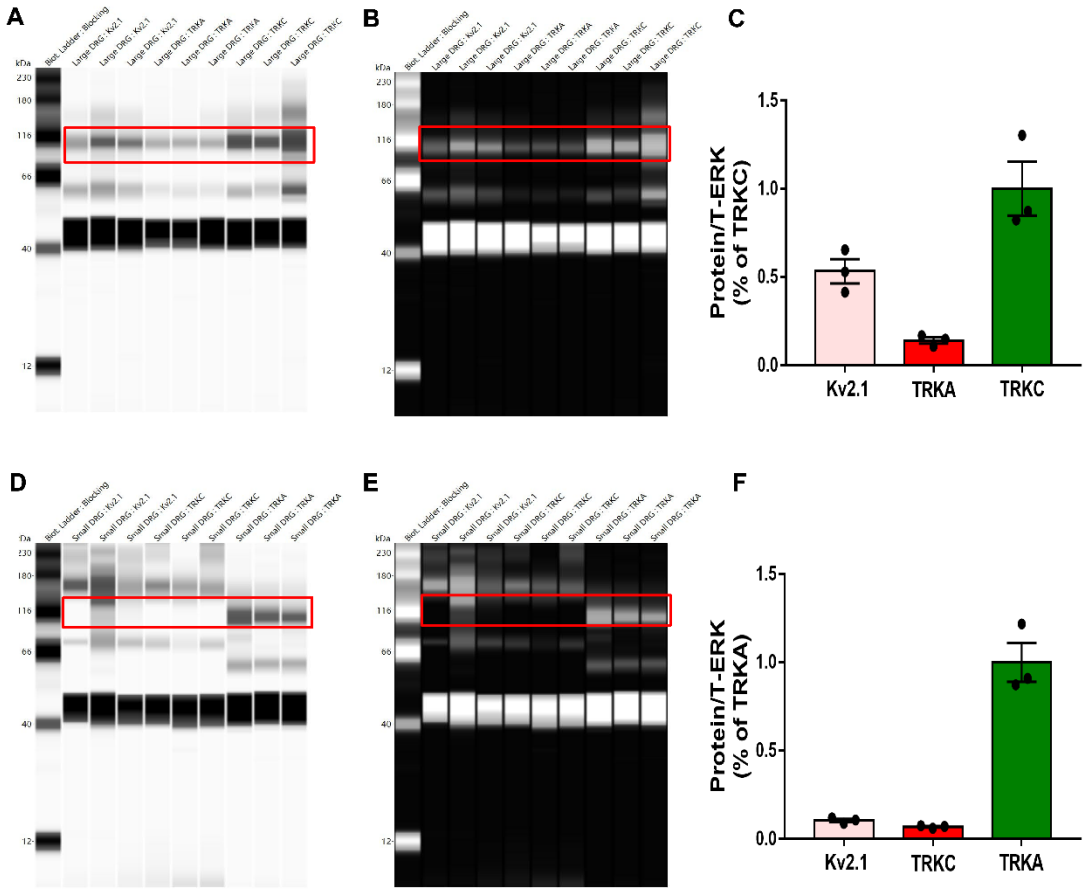

Supplemental Fig. S8. Kv2.1 expression in small, medium and large DRG neurons of DPN mice, related to Figure 2.

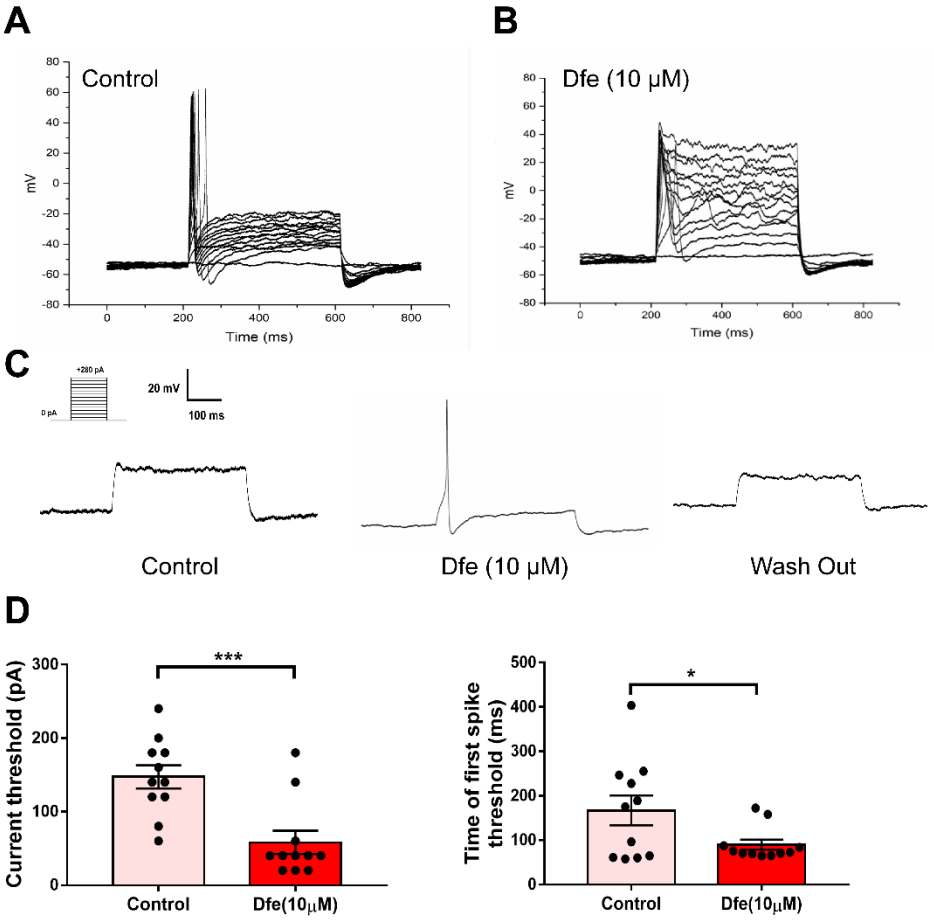

Supplemental Fig. S9. Example traces of the action potential and distribute images of single action potential of Dfe, related to Figure 2.

A

Time (h)	Concentration of Dfe in plasma (ng/ml)
0.25	22.14
1.5	30.38
4	2.46
8	-1.64
12	-1.86
24	-2.28

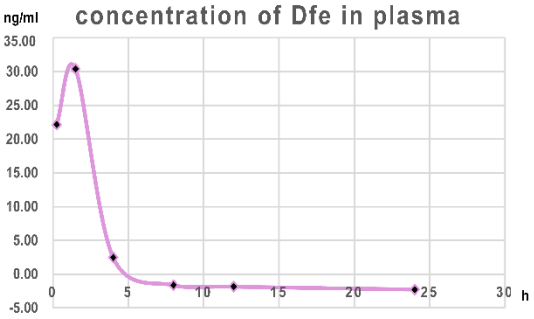

B

Time (h)	Concentration of Dfe in DRG (ng/ml)
0.25	7.96
1.5	8.76
4	3.33
8	0.55
12	-0.31
24	-0.38

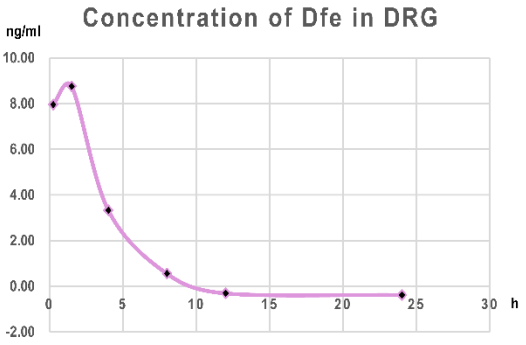

Supplemental Fig. S10. The concentration of Dfe in plasma and DRG tissue, related to Figure 1.

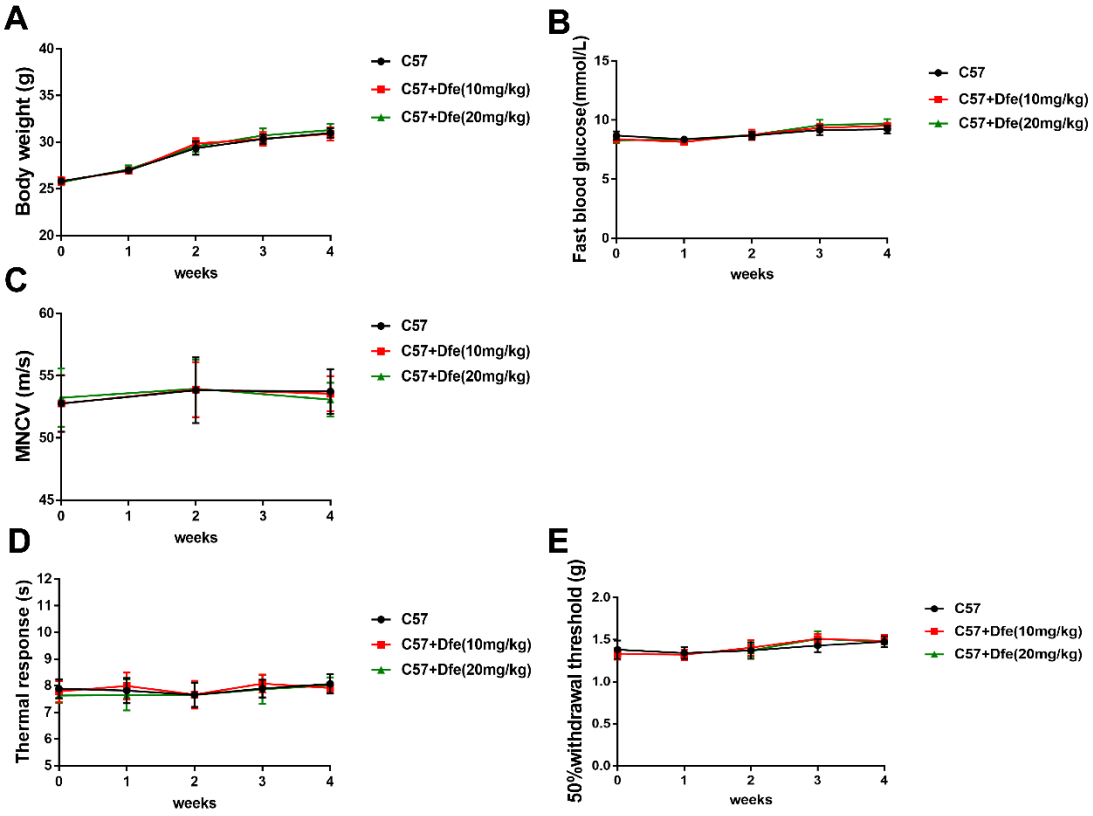

Supplemental Fig. S11. Time course of body weight and fast blood glucose in normal mice, related to Figure 4.

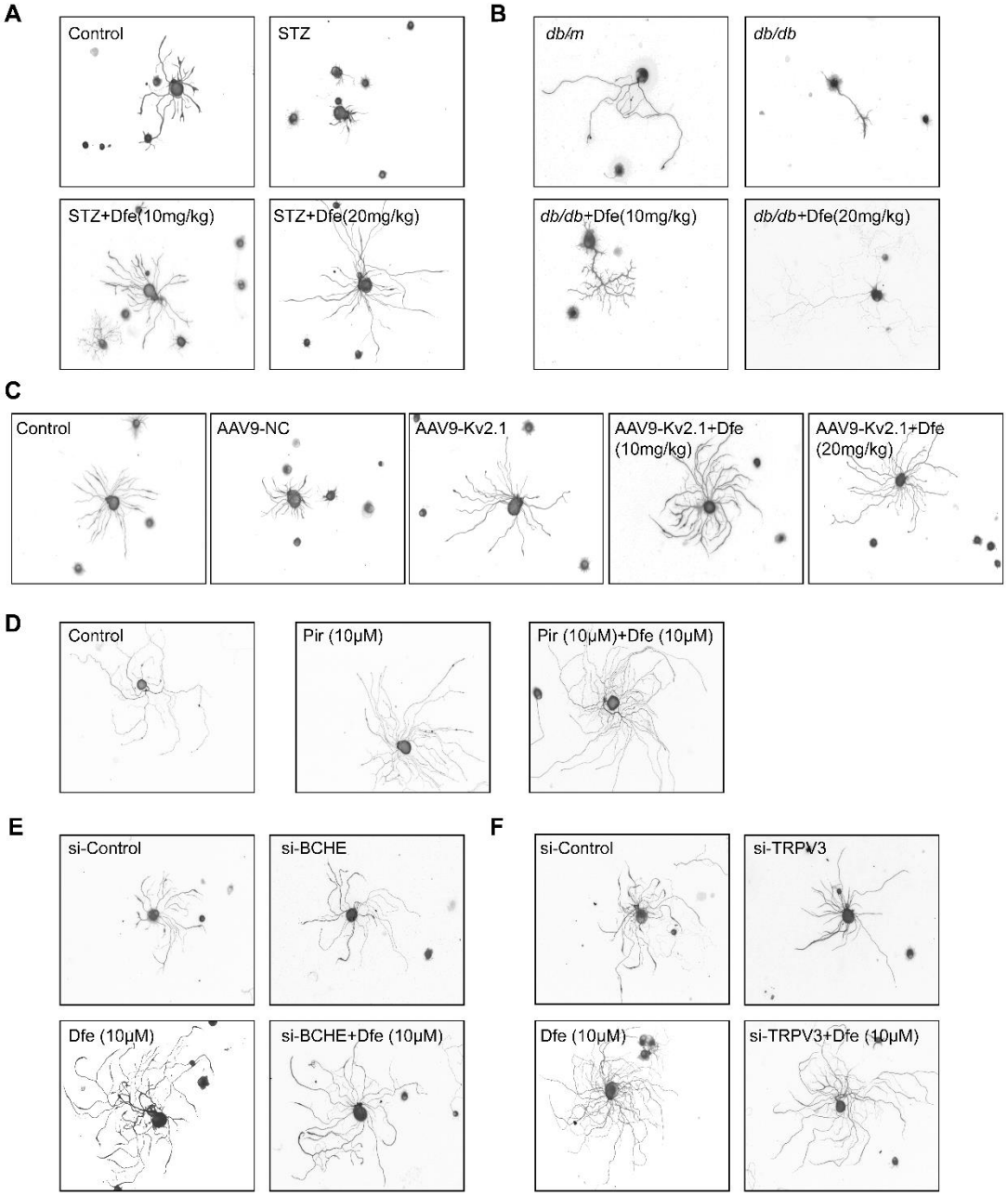

Supplemental Fig. S12. Grayscale images of neurites in DRG neurons from DPN mice, related to Figure 3.

Supplemental Table 1. List of Kv2.1-siRNA interference sequences used in real-time RT-PCR, related to Figure 3-8.

si-RNA	Target sequence
si-RNA1(si-1)	AGCAGAGGTAATTATAATCCA
si-RNA2(si-2)	CAGAGTCTGACAGAACTCCTA
si-RNA3(si-3)	TGGGTGGGTTATATGCTCATA
si-RNA4(si-4)	TACCCGAACCACTATCTTCTA

Supplemental Table 2. List of BCHE-siRNA interference sequences used in Western Blot, related to Figure 3.

si-RNA	Target sequence
si-RNA1(si-1)	CCGCAACCCUUAAACAAAUTT AUUUGUUUAAGGGUUGCGGTT
si-RNA2(si-2)	GCUCGUGUUGAAAGAGUUATT UAACUCUUUCAACACGAGCTT
si-RNA3(si-3)	GGGAGUUAACAAAGAUGAATT UUCAUCUUUGUUAACUCCCTT

Supplemental Table 3. List of TRPV3-siRNA interference sequences used in Western Blot, related to Figure 3.

si-RNA	Target sequence
si-RNA1(si-1)	CCAAGAAGAGUGCACACUUTT AAGUGUGCACUCUUCUUGGTT
si-RNA2(si-2)	GCUCCUAGGGAGGAUGUUUTT AAACAUCCUCCCUAGGAGCTT
si-RNA3(si-3)	CCUGUCAGAUGCCUGGUUUTT AAACCAGGCAUCUGACAGGTT

Supplemental Table 4. List of primers used in real-time RT-PCR, related to Figure 2.

Gene	Forward Primer	Reverse Primer
Kv1.1	GGAGCGCCCCCTACCCGAGAAG	GGTGAATGGTGCCCGTGAAGTCCT

Kv1.2	TCCCGGATGCCTTCTGGTG	GGCCTGCTCCTCTCCCTCTGT
Kv1.4	TTGTGAACGCGTGGTAATAAATGTGT	GGCGGCCTCCTGACTGGTAATAATA
Kv2.1	TCGACAACACGTGCTGTGCT	GGCCAACTTCAGGATGCGC
Kv2.2	TTGATAACACCTGCTGCCCG	TGGCGAGTTTCAGTATCCTGA
Kv3.4	CCACGGGGCAATGACCACACC	ACACAGCGCACCCACCAGCATTCCT
Kv4.2	GCCGCAGCGCCTAGTCGTTACC	TGATAGCCATTGTGAGGGAAAAGAGCA
Kv4.3	CTCCCTAAGCGGCGTCCTGGTCATT	CTTCTGTGCCCTGCGTTTATCTGCTCTC
Kv5.1	CTGGTGGGCTATCATCACCA	CGGGTCCTATGATGCTTCTC
Kv6.1	GTCCGTTCTGTTTGTCACCG	GGATCAGCACCCGTTCTTGT
Kv6.2	GGCTCTTCGCCTACGTCTC	CATCACGCGTGCTGTCCTC
Kv8.1	TCTGCGCATGCTGAAACTGG	AGTACTTGCTCTCTCCCTGC
Kv8.2	CTTCCGAATCCTCAAGCTGG	GTTGACCTTTCCTCGTTCCC
Kv9.1	AGGTAGTGCAAGTGTTCCGC	AAGTCCTCAAACTCGCGCTG
Kv9.2	TTCTCAAGCTGGCCAGACAC	TGACCGAAGGGACCTCTTTC
Kv9.3	TGTAGGGCTTCGGTCTCTTG	AGTACGGTAGCTCATGGCAC

KEY RESOURCES TABLE

REAGENT or RESOURCE	SOURCE	IDENTIFIER
Antibodies		
Rabbit anti-phospho AMPK(Thr172)	Cell Signaling Technology	Cat# 8208; RRID: AB_1658160
Rabbit anti-total AMPK (T-AMPK)	Cell Signaling Technology	Cat# 5831; RRID: AB_10622186
Rabbit anti-CaMKKβ	Santa Cruz Biotechnology	Cat# SC-50341; RRID: AB_2068532
Rabbit anti-phospho ACC	Cell Signaling Technology	Cat# 11818; RRID: AB_2687505
Rabbit anti-PGC-1α	Abcam	Cat# ab54481; RRID: AB_881987
Mouse anti-Kv2.1	Abcam	Cat# ab192761; RRID: N/A
Rabbit anti-PGP9.5	Abcam	Cat# ab108986; RRID: AB_10891773
Rabbit anti-Bcl-xl	Cell Signaling Technology	Cat# 2764; RRID: AB_2228008
Rabbit anti-Bax	Cell Signaling Technology	Cat# 5023; RRID: RRID: AB_10557411
Rabbit anti-Caspase-3	Cell Signaling Technology	Cat# 14220; RRID: AB_2798429
Rabbit anti-Cleaved caspase-3	Cell Signaling Technology	Cat# 9664; RRID: AB_2070042
Rabbit anti-iNOS	Cell Signaling Technology	Cat# 13120; RRID: AB_2687529
Rabbit anti-P-IκBα	Cell Signaling Technology	Cat# 2859; RRID: AB_561111

Rabbit anti-P-Bad	Cell Signaling Technology	Cat# 5284; RRID: AB_560884
Mouse anti-Bad	Cell Signaling Technology	Cat# 9239; RRID: AB_2062127
Rabbit anti-TNF-α	Cell Signaling Technology	Cat# 11948; RRID: AB_2687962
Rabbit anti-Total extracellular regulated protein kinase (T-ERK)	Cell Signaling Technology	Cat# 9102; RRID: AB_330744
Rabbit anti-NeuN	Cell Signaling Technology	Cat# 24307; RRID: AB_2651140
Anti-mouse IgG, HRP-linked Antibody	Cell Signaling Technology	Cat# 7076; RRID: AB_330924
Anti-rabbit IgG, HRP-linked Antibody	Cell Signaling Technology	Cat# 7074; RRID: AB_2099233
fluorescein 596-conjugated secondary antibody	Proteintech	Cat# SA00013-4; RRID: AB_2810984
fluorescein 488-conjugated secondary antibody	Proteintech	Cat# SA00013-1; RRID: AB_2810983
Virus Strains		
AAV9-Kcnb1-RNAi	GENECHEM	Cat# 77626-1
AAV9-CON400	GENECHEM	N/A
Chemicals, Peptides, and Recombinant Proteins		
Fetal Bovine Serum (FBS)	ThermoFischer Scientific	Cat# 10100
B27 serum-free supplement	ThermoFischer Scientific	Cat# 17504044
Drofenine Hydrochloride	Absin	Cat# 819384
Ham's F-12 Nutrient Mix	ThermoFischer Scientific	Cat# 11765054
REAGENT or RESOURCE	SOURCE	IDENTIFIER
Penicillin-Streptomycin	ThermoFischer Scientific	Cat# 15140148
Dulbecco's Modified Eagle's Medium	Hyclone	Cat# SH30022.01B
Puromycin	Beyotime	Cat# ST551
RIPA Lysis Buffer	Beyotime	Cat# P0013D
Collagenase from Clostridium histolyticum	Sigma-Aldrich	Cat# C0130
Poly-d-Lysine (PDL)	Solarbio	Cat# D6790
4% paraformaldehyde	Solarbio	Cat# P1110
Toluidine Blue O	Solarbio	Cat# G3661
Dimethylsulfoxide	Sigma-Aldrich	Cat# D2650
Streptozotocin	Sigma-Aldrich	Cat# S0130
Polysorbate 80	Sigma-Aldrich	Cat# 59924
viscous liquid	Sigma-Aldrich	Cat# P7949
Sodium pyruvate	Sigma-Aldrich	Cat# 792500
L-Glutamine	Sigma-Aldrich	Cat# G3126
Thiazolyl Blue Tetrazolium Bromide	Sigma-Aldrich	Cat# M2128
Carbonyl cyanide 4-(trifluoromethoxy) phenylhydrazone	Sigma-Aldrich	Cat# C2920
Rotenone	Sigma-Aldrich	Cat# R8875
Lipofectamine 2000 Transfection Reagent	ThermoFischer Scientific	Cat# 11668019

Protease Inhibitor Cocktail (100X)	ThermoFischer Scientific	Cat# 78430
Protease and Phosphatase Inhibitor Cocktail (100X)	ThermoFischer Scientific	Cat# 78444
Oligomycin A	Broadway	Cat# 325839
PrimeScript (R) RT Master Mix	Takara Bio	Cat# RR036B
RNAiso Plus	Takara Bio	Cat# 9109
Dispase II	ThermoFischer Scientific	Cat# 17105041
Critical Commercial Assays		
BCA protein assay kit	Beyotime	Cat# P0012
Mitochondrial membrane potential assay kit with JC-1	Beyotime	Cat# C2006
Seahorse XF Cell Mito Stress Test kit	Agilent Technologies	Cat# 102416-100
One Step TUNEL Apoptosis Assay Kit	Beyotime	Cat# C1088
TNFα ELISA Kit	Nanjing Jiancheng Bioengineering Institute	Cat# H052
IL-6 ELISA Kit	Nanjing Jiancheng Bioengineering Institute	Cat# H007
IL-1β ELISA Kit	Nanjing Jiancheng Bioengineering Institute	Cat# H002
REAGENT or RESOURCE	SOURCE	IDENTIFIER
HE Staining Kit	Solarbio	Cat# G1120
DAB Kit	ZSGB-BIO	Cat# ZLI-9017
Experimental Models: Cell Lines		
CHO-Kv2.1	CLS	Cat# 603480/p693; RRID: CVCL_0214
CHO-K1	CLS	Cat# 603480/p693; RRID: CVCL_0214
Experimental Models: Mouse		
Mouse: C57BL/6	Beijing Vital River Laboratory Animal Technology Co., Ltd.	N/A
Mouse: BKS Cg-*m*$^{+/+}$*Lepr*^{db}/*J*	Model Animal Research Center of Nanjing University	N/A
Oligonucleotides		
Primers: mouse Kv2.1 Forward: TCGACAACACGTGCTGTGCT Reverse: GGCCAACTTCAGGATGCGC	Sangon Biotech	N/A

Primers: mouse β-actin Forward: TCATCACTATTGGCAACGAGC Reverse: AACAGTCCGCCTAGAAGCAC	Sangon Biotech	N/A
Kv2.1 si-RNA	QIAGEN	Cat# 1027416
Recombinant DNA		
Plasmid: pLV-EYFP-N-Kv2.1	Yao XG et al., 2013	N/A
Plasmid: pcDNA3.1a-Kv2.2	Zhou TT et al., 2016	N/A
Software and Algorithms		
GraphPad Prism 7 software	GraphPad Inc.	https://www.graphpad.com
Image J	Image J	RRID: SCR_003070

Transparent methods

1. Animals

All animals were received humane care and housed in standard cages and maintained on a 12-h light/dark cycle at an ambient temperature of 22°C. Animal-related protocols were approved by the Institutional Animal Care and Use Committees at Nanjing University of Chinese Medicine. Male C57BL/6 mice at 7 weeks of age were purchased from Beijing Vital River Laboratory Animal Technology Co., Ltd., and male BKS Cg-m+/+Leprdb/J *db/db* mice aged 17 weeks were purchased from Model Animal Research Center of Nanjing University.

Type 1 diabetic mice with DPN-Type 1 diabetic mice with DPN (STZ) were prepared according to the literature approach (Emiri et al., 2019). Briefly, seven-week-old male C57BL/6 mice were fed adaptively for one week and then induced by a single

intraperitoneal injection of STZ (Sigma Aldrich) at 150 mg/kg. Nondiabetic mice (Control, used as control animals in STZ mice-related assay. N = 12) were injected with 200 μl vehicle buffer (Na-Citrate Buffer, pH 4.5). Type 1 diabetic mice were defined as a fasting blood glucose level >16 mmol/L after STZ injection one week (Ma et al., 2014). Motor nerve conduction velocity (MNCV) was detected at Week 0, 4 and 10 post STZ injection, tactile allodynia and thermal sensitivity were detected every week and Drofenine was administrated at Week 7, 8, 9 and 10. DPN mice were defined at 12 weeks of age (4 weeks after STZ injection) through behavioral tests (insensitivity to mechanical stimulation, thermal hypoalgesia and decreased motor nerve conduction velocity, *etc*.).

Type 2 diabetic mice with DPN-Type 2 diabetic mice with DPN were prepared according to the published approach (Menichella et al., 2014) and *db/db* mice aged 18 weeks were used as type 2 diabetic mice with DPN (*db/db*). Age-matched heterozygotes mice (*db*/m) with nonpenetrant genotype were used as control animals in *db/db* mice-related assay. MNCV was detected at Week 0, 2 and 4, tactile allodynia and thermal sensitivity were detected every week and Drofenine was administrated at Week 1, 2, 3, and 4.

Normal mice-Fifteen-week-old male C57BL/6 mice were applied for the experiment. Dfe (10, 20 mg/kg) was administered by intraperitoneal injection for four weeks. Body weight and fast blood glucose of mice were measured every week, and tactile allodynia, MNCV and thermal sensitivity were monitored every week.

2. AAV9-Kv2.1-RNAi vector injection

In the current work, AAV was used in knockdown related experiments for its safety and high infection efficiency *in vivo* (Fang et al; 2012). By considering that type 1

diabetic mice may exhibit more obvious DPN-like symptoms compared with type 2 diabetic mice (Otto-Buczkowska et al., 2008; Sima et al., 2006), type 1 diabetic mice were here chosen for AAV-related assay.

For constructing adeno-associated-virus (AAV) 9-Kv2.1-RNAi, a gene sequence (5' to 3': (RNA)-CAG AGT CTG ACA GAA CTC CTA) able to significantly knock down the protein expression of Kv2.1 channel was at first *in vitro* screened in DRG neuron (Fig. S5A and B). AAV carrying the target gene was constructed in Shanghai Genechem Co., Ltd. Shanghai, China. The titer of AAV9-Kv2.1-RNAi vector was 1.29 $\times 10^{13}$ vector genomes/ml. It was diluted with saline to reach the titer of 1.7×10^{11} vector genomes/mouse. Two weeks after tail vein injection of the virus into STZ mice, mRNA and protein expression levels of Kv2.1 channel in DRG tissue were detected by RT-PCR and western blot (Fig. S5C and D).

3. Animal administration

Dfe was dissolved in physiological saline with 2% DMSO and 8% tween 80 (Vehicle buffer). STZ, *db/db* or AAV9-Kv2.1-RNAi injected STZ mice (N = 12) were daily administrated with 10 or 20 mg/kg of Dfe by intraperitoneal injection for 4 weeks. Control (N = 12) or *db/m* (N = 12) mice were administrated with the same volume of the vehicle buffer as that for DPN mice. Mice were sacrificed 4 weeks after the last administration of Dfe under sodium pentobarbital (5 mg/100g) anesthesia.

4. Weight and glucose measurements

Measurements of body weight and blood glucose levels in mice were conducted weekly according to published methods (Roy Chowdhury et al., 2012). Fasting blood glucose was obtained from tail vein using a blood glucose meter (Roche).

5. Tactile allodynia test

Tactile allodynia test was carried out according to the published approach

(Chaplan et al., 1994). Von Frey filaments were purchased from Ugo Basile, Comerio VA, Italy. A paw withdrawal of mice in response to each irritation was recorded. Each mouse was measured six times to determine the threshold, and 50% withdrawal threshold was calculated according to 50% threshold= (10^ (xf + kδ)/10,000.

6. Thermal sensitivity measurement

Thermal sensitivity measurement was carried out according to the published approach (Wang et al., 2011). Plantar thermal stimulation meter was purchased from Ugo Basile, Comerio VA, Italy. Briefly, mice were placed in a perspex enclosure with a metal mesh floor, and a movable radiant heat source was placed directly under the plantar surface of the hind paw. The paw withdrawal latency was automatically recorded from the onset of irradiation (Lamp 40 W, distance lamp to paw 40 mm, 24°C room temperature) to the withdrawal of the hind paw. The average withdrawal time of the left and right hind paws was used for statistical analysis.

7. Neurophysiological measurement

Neurophysiological measurement was carried out according to the published approaches (Wang et al., 2012; McGuire et al., 2009; Kumar et al., 2007). Mice were placed on a heated pad in a room maintained at 25°C to ensure a constant rectal temperature at 37°C. After mice were treated with intraperitoneal injection of sodium pentobarbital (5 mg/100g), the motor nerve conduction velocity (MNCV) of sciatic nerve ranging from ankle to sciatic notch was measured via bipolar electrodes with a supramaximal stimulus (3V) of 0.05 ms duration. MNCV was measured by dividing the distance between the distal and proximal ends. Calculation formula was set by: nerve conduction velocity (m/s) = distance between two points (cm) *10/latency difference between two points.

8. Measurement of regional blood flow velocity and perfused blood vessel area

Mice in each group were anesthetized with isoflurane inhalation (small animal anesthetic machine, RWD, China). The real-time regional velocity, blood flow distribution and perfused blood vessel of sciatic nerve and foot pads were detected by Laser Speckle Contrast Imaging/LSCI (RFLSI Pro, RWD, China). Regional sciatic nerve and foot pad blood flow ratios from control mice were used as baseline values. The imaging system presented blood perfusion signal with a color-coded image ranging from dark blue (low perfusion) to bright red (high perfusion). When observing the blood flow of sciatic nerve, the signal interference of surrounding tissue should be avoided as much as possible. 100 consecutive photographs were taken, and blood flow velocity and blood perfusion area were analyzed by BFI software and Image J.

9. Cell Culture

CHO cell was cultured in Dulbecco's Modified Eagle Medium (DMEM) with 10% FBS, 100 U/ml penicillin and 100 μg/ml streptomycin with 5% CO_2 at 37°C. CHO-Kv2.1 cell was cultured in DMEM medium containing 0.25 μg/ml purinomycin, 10% FBS, 100 U/ml penicillin and 100 g/ml streptomycin with 5% CO_2 at 37°C.

Primary sensory neuron (dorsal root ganglion, DRG) from adult male mice were cultured in Ham's F-12 containing 1% PS and 2% B27 based on the published approach (Roy Chowdhury et al., 2012). In all studies, neuron from normal mice was grown in defined Hams F12 medium with B27 additive including 10 mM D-glucose and 10 nM insulin, and neuron from DPN mice was maintained in medium containing 25 mM D-glucose (Gavazzi et al., 1999; Roy Chowdhury et al., 2012).

10. Kv2.1 channel inhibitor screening

Kv2.1 channel inhibitor screening was performed based on our previously published approach (Zhou et al., 2016). Briefly, the CHO cell overexpressing Kv2.1

was co-incubated with compounds in voltage-sensitive fluorescent indicators and membrane dyes. Fluorescent indicators were attached to the outside of the cell membrane and covered by membrane dyes. In the process of screening compounds, compounds were added into cell at 1:1000 and then dyed at 1:1. The compounds, dyes and cells were incubated for 30 minutes before addition of KCl (100 mM). Membrane potential assay was conducted by Flex station III instrument (Molecular Devices). The changes of potential energy were observed. Kv2.1 inhibitor was evaluated by comparison with negative control (DMSO). To exclude the effect of the discovered inhibitor on the other ion channels, the effects of compounds on potential energy were detected in normal CHO cell.

11. Electrophysiological recording assay

The whole-cell patch clamp recordings against cultured CHO-Kv2.1 cell or DRG neuron were performed at room temperature with Axopatch-200B amplifier (Molecular Devices) as described previously (Li et al., 2005). The microelectrodes fashioned from 1.5 mm thin-walled borosilicate glass with filament were pulled from Flaming/Brown type micropipette puller (P-97; SUTTER INSTRUMENT). Pipettes had resistances of 3-7 MΩ when filled with a solution as following composition: for CHO-Kv2.1 cell, 140 mM KCl, 2 mM $MgCl_2$, 10 mM EGTA, 1 mM $CaCl_2$, 10 mM HEPES (pH 7.3); for DRG neuron, 135 KCl, 3 Mg-ATP, 0.5 Na_2-ATP, 1 $CaCl_2$, 2 EGTA, 5 Glucose (pH7.3-7.4). Cell was bath perfused with a solution of the following composition: for CHO-Kv2.1 cell, 150 mM NaCl, 5 mM KCl, 0.5 mM $CaCl_2$, 1.2 mM $MgCl_2$, 10 mM HEPES (pH 7.3); for DRG neuron, 140 mM NaCl, 4 mM KCl, 2 mM $CaCl_2$, 2 mM $MgCl_2$, 10

mM HEPES, 10 mM Glucose (pH 7.3-7.4). The current signals were filtered at 1 kHz and digitized at a 10 kHz sampling frequency by using DigiData 1440 A (Molecular Devices) and analyzed with the software of pClamp 10.2 (Molecular Devices). Whole-cell currents were recorded using the protocol as follows: the holding potential was set at -80mV (for CHO-Kv2.1 cell) or -100 mV (for DRG neuron), and stepwise depolarized from -80 to 120 mV in 20 mV (for CHO-Kv2.1 cell) or -60 to +50 mV in 10 mV (for DRG neuron) increments and then repolarized to -60 mV (for CHO-Kv2.1 cell) or -100 mV (for DRG neuron). For large cell, we further performed the correction offline by recording much of empty control CHO cell (Li et al., 2002). Liquid junction potentials were less than 2 mV, and calculated using JPCalc software (Barry et al., 1994).

To record action potential, a current clamp protocol delivered several hyperpolarizing steps of increasing amplitude (20 pA increments, 400 ms duration, -50 mV holding potential) from 0 pA to 280 pA.

12. Liposome transfection assay

CHO cell was inoculated in 96-well plates, after 24 hours of culture the original culture medium was replaced by that without serum and antibiotics. Lipofectamine 2,000 was used to transfect pcDNA3.1a-Kv2.2 plasmid (1,000 ng/well) into CHO cell. Then, the cell culture medium was replaced by complete medium after 6 hours of transfection followed by overnight incubation in incubator, and subsequent experiments were carried out.

The liposome transfection assay procedures for BCHE si-RNA and TRPV3 si-RNA (1,000 ng/well) in DRG neuron were similar to those above-mentioned

approaches.

13. MTT assay

Viability of cultured cell was detected by MTT assay. Briefly, CHO-Kv2.1 cell was seeded overnight in 96-well plates at a density of 10^5 cell/well in 100 μL medium, and co-incubated with different concentrations of Dfe (5, 10, 20 μM) for 24 h. The medium was removed and added with 0.5 mg/μL MTT. After incubation at 37°C for 4 h, 100 μL of dimethyl sulfoxide (DMSO) was added to each well, and the mixture was shaken at a low speed for 10 min on a shaker to fully dissolve the formazan crystals, followed by the measurement of absorbance at 490 nm using an MI3X spectrophotometer (Molecular Devices).

14. Total neurite outgrowth assessment

Detection of neurite outgrowth was carried out by the published approach (Roy Chowdhury et al., 2012). DRG neuron from adult male mice was inoculated into a 12-well plate at 100 cell per well. After overnight adherence, cell was incubated with different concentrations of Dfe (5, 10, 20 μM) for 24 hours. The original culture medium was removed and fixed with 4% polyformaldehyde for 15 minutes, and 0.3% Triton was permeated for 5 minutes, then washed by PBS and sealed at room temperature for 1 hour. β-tubulin III antibody (1:1000; Sigma Aldrich) was incubated overnight (1:1000) at 4°C and then incubated with goat anti-mouse (1:200; Proteintech) at room temperature for 1 hour. Finally, imaging was captured under a fluorescence microscope. As shown in Fig. S11, Image J (Meijering et al., 2010) was used to quantify the neurite outgrowth of DRG neuron based on the grayscale images. Neurite picture

was at first converted to grayscale, and the background signal was subtracted. All neurites were traced and measured by freehand using Image J.

15. Mitochondrial membrane potential assay

Mitochondrial membrane potential (MMP) assay was carried out by the manufacturer's protocol (Srinivasan et al., 2000). Briefly, DRG neurons from normal mice, DPN mice or Dfe-treated DPN mice were plated in 96-well plates at a density of 20,000 cell/well and incubated for 24 h, followed by incubation with JC-1 solution (Beyotime) at 37°C in an environment protected from light for 20 min. Then, cells were washed with Hams F12 without FBS, and fluorescence data were analyzed with Microplate Reader (MD, USA). Ratio of green/red (530/590 nm) fluorescence was used as an indicator of MMP.

16. Measurement of mitochondrial respiration in DRG neuron

DRG neuron was seeded into a specialized 96-well microplates allowing for oxygen consumption rates (OCR) monitored in real time at 20,000 cell per well (Hill et al., 2009). An XF96 Analyzer (Seahorse Biosciences) was preheated at 37°C overnight the day before, and calibration solution was added into the Utility plate, followed by hydration overnight in an incubator (CO_2 free) at 37°C. Base Medium and detection solution were prepared the next day, and the required substrates (Glutamine, Glucose, Pyruvic Acid) were added. ATP synthase inhibitor Oligomycin (1 μM), uncoupling agent carbonyl cyanideptrifluorocarbonyl-cyanide methoxyphenyl hydrazine (FCCP) (0.75 μM) and respiratory chain inhibitor rotenone/antimycin A (ROT/AA) (1 μM, 1:1) were injected sequentially after medium exchange. The results were obtained after

approximately 80 minutes and analyzed using wave software. The difference of control values might be caused by the calibration of the instrument itself (Calcutt et al., 2017; Chowdhury et al., 2013).

17. Immunofluorescence

Cultured cell-based assay

DRG neuron from STZ or *db/db* mice was cultured in 12-well plate at 37°C for 24h and then fixed in 4% paraformaldehyde for 24 hours at room temperature. Annexin V/PI double staining was used to detect cell apoptosis. Images were collected under a 10-fold microscope using fluorescence microscope (Leica), Leica quantitative software was used to analyze and quantify the results.

Tissue-based assay

Sciatic nerve, epidermal foot pad and DRG tissues of mice were used for immunohistochemistry assay according to the published approach (Wang et al., 2011).

Measurement of density of intraepidermal nerve fibers (IENFs)- The epidermal foot pad tissue of mice was removed and fixed in 4% paraformaldehyde for 24 hours at room temperature. The foot pad tissue was embedded in paraffin and then cut into 6 μm-thick sections in microtome. Sections were incubated overnight at 4°C with primary antibody PGP 9.5 (1:1000; Abcom) diluted in blocking solution of 3% goat serum, followed by incubation with HRP (Horseradish peroxidase)-conjugated secondary antibody (Yeasen Biotech Co., Ltd) the next day at 37°C for 1h. Sections were washed in PBS, and DAB staining (Zsbio) was then applied to label positive intraepidermal nerve fibers. Nuclei were counter-stained with Hematoxylin (Solarbio). Images were collected under a light

microscope at 40 × magnification (Leica). Morphometric analyses were performed by IHC-Toolbox in Image J (Abramoff et al., 2004).

Measurement of myelin sheath of sciatic nerves- Sciatic nerve tissue of mice was removed and fixed in Glutaraldehyde (Solarbio) for 24 hours at room temperature. It was embedded in paraffin and then cut into 2 μm-thick sections in microtome. Sections were stained with toluidine blue to analyze the area of myelin sheath. The fields were chosen randomly, and images were collected under a light microscope at 100 × magnification (Leica). Morphometric analyses were performed by IHC-Toolbox in Image J (Abramoff et al., 2004).

Detection of apoptosis in DRG tissue-DRG tissue of mice was removed and fixed in 4% paraformaldehyde for 24 hours at room temperature. It was embedded in paraffin and then cut into 6 μm-thick sections in microtome. Sections were incubated overnight at 4°C with primary antibody NeuN (1:1000; Cell Signaling Technology) diluted in blocking solution of 3% goat serum, followed by incubation with fluorescein 596-conjugated secondary antibody (1:200, anti-rabbit, Proteintech) and tunnel (Beyotime) the next day at 37°C for 1h. Images were collected under a 63-fold microscope using laser scanning confocal microscope (Leica), leica quantitative software was used to analyze and quantify the results.

Detection of the number of NF-kB entering nuclei in DRG tissue-DRG tissue of mice was removed and fixed in 4% paraformaldehyde for 24 hours at room temperature. It was embedded in paraffin and then cut into 6 μm-thick sections in microtome. Sections were incubated overnight at 4°C with primary antibody β-tubulin III (1:1000;

Sigma Aldrich) and NF-κB (1:1000; Abcam), followed by incubation with fluorescein 596-conjugated secondary antibody and fluorescein 488-conjugated secondary antibody the next day at 37°C for 1h. Hoechst was used as a marker of nucleus. Images were collected under a 63-fold microscope using laser scanning confocal microscope (Leica). A single channel-based quantification was performed by using Leica software and the fluorescence intensity in the nucleus was focused.

Detection of the area of Kv2.1 expression in DRG tissue- DRG tissue of mice was removed and fixed in 4% paraformaldehyde for 24 hours at room temperature. It was embedded in paraffin and then cut into 6 μm-thick sections in microtome. Sections were incubated overnight at 4°C with primary antibody Kv2.1, followed by incubation with HRP (Horseradish peroxidase)-conjugated secondary antibody was carried out at 37°C for 1h. DAB staining was then applied to label Kv2.1. Nuclei were counter-stained with Hematoxylin. Images were collected under a light microscope at 100 × magnification (Leica). Morphometric analyses were performed by IHC-Toolbox in Image J (Abramoff et al., 2004).

18. RT-PCR analysis

Total RNA of DRG tissue in mice was extracted by TRIzol reagent. 1 μg mRNA was used to reverse transcribe into cDNA, and the reverse transcriptional procedure was at 37°C for 15 min. cDNA was detected using SYBR Premix Ex Taq kit and a Bio-Rad CFX connect real-time system machine. Results were normalized to mRNA levels of β-actin.

19. Western blot assay

Protein samples were obtained from DRG tissue of mice. SDS-PAGE sampling buffer (25% SDS, 62.5mM Tris, 25% glycerol, 0.1% bromofenblue, pH 6.8) was used for protein collection. Proteins were electrophoretized, transferred and blocked, while incubated with antibodies to the following proteins (KEY RESOURCES TABLE). Total extracellular regulated protein kinase (T-ERK) was used as a loading control for its good stability in DRG tissue (Fernyhough et al., 1999; Calcutt et al., 2017). Finally, the horseradish peroxidase (HRP) substrate was incubated for 5 minutes, and the signals were collected using the Tanon-5200 Multi luminescent imaging system. Quantity One software was used for all protein band quantification.

20. Jess-based analysis of protein

Protein samples were obtained from DRG tissue of STZ mice. After digestion, DRG neuron was filtered by 40 μM cell sieve, and large and small DRG neurons were isolated. Samples were run undilutedly on a 12-230 kDa separation module according to the manufacturer's instructions. Data were analyzed with Compass software version 4.0.0 (ProteinSimple). For analysis on the Jess system from ProteinSimple, antibodies of anti-Kv2.1 (Abcam; ab192761; 1:50), anti-TRKA (Bioss; bs-0193R; 1:50), anti-TRKC (Proteintech; 111999-1-AP; 1:50) and anti-ERK (Cell Signaling Technology; 9102; 1:200) were used.

21. Pharmacokinetic analysis of Dfe

Dfe level in DRG tissue or plasma of mice was detected by using a Thermo TSQ Vantage tandem mass spectrometer coupled with an HPLC model U3000 apparatus (Dionex, San Jose, CA). Dfe was administered intraperitoneally (20 mg/kg) in normal

mice. Blood was taken from the orbit at 0 min, 15 min, 90 min, 4 h, 8 h, and 12 h after administration. DRG tissue was taken at 0 min, 15 min, 90 min, 4 h, 8 h, 12 h, and 24 h after administration. Blood was placed in a tube prepared in advance with heparin sodium (0.3% heparin sodium, 10 μL), and then centrifuged at 8,000 rpm at 4°C for 5 min. The upper plasma was transferred to a pre-cooled EP tube and stored at 4°C for testing. DRG tissue was taken into a 1.5 mL EP tube containing 1 mL of saline in advance, and then centrifuged at 4,000 rpm for 2 minutes to discard the upper saline. DRG tissue in each tube was weighted and stored at -20°C. Methanol was used to precipitate protein and extract analyte, and Dfe concentration in plasma or DRG tissue was assessed by LC-MS/MS.

22. ELISA assay

Inflammatory cytokines IL-6, IL-1β and TNFα in the serum of mice were quantified according to mouse ELISA kit instructions (Nanjing Jiancheng Bioengineering Institute). Samples of mouse serum were separately incubated in a plate coated with TNFα, IL-6, IL-1β antibody at 37°C for 30 minutes, and then HRP secondary antibody was added and incubated at 37°C for 30 minutes. Next, solution A and solution B were added and incubated for 10 minutes, and finally the stop solution was added to stop the reaction. Normal color development and reading protocol as per ELISA plate reader manufacturer's directions were followed.

23. Data analysis

All experiments performed were blind to group assignment. All data in the current work were plotted, analyzed by GraphPad Prism 7 software (except for special

instructions) and shown as mean ± sem. Unpaired 2-tailed Student's t test was used for two-group comparison. One-way ANOVA with post hoc comparisons using Tukey's or Dunnett's post hoc tests was used for at least three groups' comparisons. P value of less than 0.05 was considered statistically significant.

Supplemental References

Abramoff, M.D., Magelhaes, P.J., and Ram, S.J. (2004). Image Processing with ImageJ. Brief. Bioinform. *11*, 36-42.

Barry, P.H. (1994). JPCalc, a software package for calculating liquid junction potential corrections in patch-clamp, intracellular, epithelial and bilayer measurements and for correcting junction potential measurements. J. Neurosci. Methods. *51*, 107-116.

Chaplan, S.R., Bach, F.W., Pogrel, J.W., Chung, J.M., and Yaksh, T.L. (1994). Quantitative assessment of tactile allodynia in the rat paw. J. Neurosci. Methods. *53*, 55-63.

Emiri MiuraTELura, Tsunekawa, S., Naruse, K., Nakamura, N., and Kamiya, H. (2019). Secreted factors from cultured dental pulp stem cell promoted neurite outgrowth of dorsal root ganglion neuron and ameliorated neural functions in streptozotocin-induced diabetic mice. J. Diabetes. Investig. DOI: 10.1111/jdi.13085.

Fang, H.F., Lai, N.C., Gao, M.H., Miyanohara, A., Roth, D.M., Tang, T., Hammond, H.K. (2012). Comparison of Adeno-Associated Virus Serotypes and Delivery Methods for Cardiac Gene Transfer. Hum Gene Ther Methods. *23(4)*: 234-241.

Gavazzi, I., Kumar, R.D.C., Mcmahon, S.B., and Cohen, J. (1999). Growth responses of different subpopulations of adult sensory neuron to neurotrophic factors. Eur. J. Neurosci. *11*, 3405-3414.

Hill, B.G., Dranka, B.P., Zou, L., Chatham, J.C., and Darley-Usmar, V.M. (2009). Importance of the bioenergetic reserve capacity in response to cardiomyocyte stress induced by 4-hydroxynonenal. Biochem. J. *424*, 99-107.

Kumar, A., Kaundal, R.K., Iyer, S., and Sharma, S.S. (2007). Effects of resveratrol on nerve functions, oxidative stress and DNA fragmentation in experimental diabetic neuropathy. Life. Sci. *80*, 1236-1244.

Li, Y., Gamper, N., Hilgemann, D.W., and Shapiro, M.S. (2005). Regulation of Kv7 (KCNQ) K+ channel open probability by phosphatidylinositol 4,5-bisphosphate. J. Neurosci. *25*, 9825-9835.

Li, Y., Hu, G.Y., and Huperzine, A. (2002). A nootropic agent, inhibits fast transient potassium current in rat dissociated hippocampal neuron. Neurosci. Lett. *324*, 25-28.

Ma, J., Farmer, K.L., Pan, P., Urban, M.J., Zhao, H., Blagg, B.S., and Dobrowsky, R.T. (2014). Heat shock protein 70 is necessary to improve mitochondrial bioenergetics and reverse diabetic sensory neuropathy following ku-32 therapys. J. Pharmacol. Exp. Ther. *348*, 281-292.

McGuire, J.F., Rouen, S., Siegfreid, E., Wright, D.E., and Dobrowsky, R.T. (2009). Caveolin-1 and altered neuregulin signaling contribute to the pathophysiological progression of diabetic peripheral neuropathy. Diabetes *58*, 2677-2686.

Meijering, E. (2010). Neuron Tracing in Perspective. Cytometry A. *77*, 693-704.

Menichella, D.M., Abdelhak, B., Ren, D., Shum, A., Frietag, C., and Miller, R.J. (2014). CXCR4 chemokine receptor signaling mediates pain in diabetic neuropathy. Mol. Pain. *10*, 42.

Otto-Buczkowska, E., Kazibutowska, Z., Sołtyk, J., Machnica, Łukasz. Neuropathy and type 1 diabetes mellitus. (2008). J. Pediatr. Endocr. Met. *4(2)*, 109-116.

Roy Chowdhury, S.K., Smith, D.R., Saleh, A., Schapansky, J., Marquez, A., Gomes, S., Akude, E., Morrow, D., Calcutt, N.A., and Fernyhough, P. (2012). Impaired adenosine monophosphate-activated protein kinase signalling in dorsal root ganglia neuron is linked to mitochondrial dysfunction and peripheral neuropathy in diabetes. Brain *135*, 1751-1766.

Sima, A.A.F., and Kamiya, H. Diabetic Neuropathy Differs in Type 1 and Type 2 Diabetes. (2006). Ann. Ny. Acad. Sci. *1084*, 235-249.

Wang, L., Chopp, M., Szalad, A., Liu, Z., and Zhang, Z.G. (2011). Phosphodiesterase-5 is a therapeutic target for peripheral neuropathy in diabetic mice. Neuroscience *193*, 399-410.

Wang, L., Chopp, M., and Zhang, Z.G. (2012). Thymosin β4 Promotes the Recovery of Peripheral Neuropathy in Type II Diabetic Mice. Neurobiol. Dis. *48*, 546-55.

Zhou, T.T., Quan, L.L., Chen, L.P., Du, T., Sun, K.X., Zhang, J.C., Yu, L., Li, Y., Wan, P., Chen, L.L., et al. (2016). Sp6616 as a new kv2.1 channel inhibitor efficiently promotes β-cell survival involving both PKC/Erk1/2 and CaM/PI3K/Akt signaling

pathways. Cell Death Dis. *7*, e2216.